

# Low-Complexity Concatenated Polar Codes with Excellent Scaling Behavior

Sung Whan Yoon, *Student Member, IEEE* and Jaekyun Moon, *Fellow, IEEE*

School of Electrical Engineering  
Korea Advanced Institute of Science and Technology  
Daejeon, 34141, Republic of Korea  
Email: shyoon8@kaist.ac.kr, jmoon@kaist.edu

**Abstract**—In this paper, highly efficient practical concatenated coding schemes with multiple short length polar codes and single-parity-check codes are proposed. As for hardware complexity, required memory space is significantly reduced by utilizing small decoding units geared to serialized decoding of short-length component polar codes. In theoretic analysis, each component short polar code shows much improved error-rate scaling-behavior thanks to simple single-parity-check decoding; the error rate decays with increasing overall code length as fast as in single stand alone code while retaining considerable hardware-memory advantage. Moreover, by applying list decoding and cyclic-redundancy-checking to each short component polar code, finite-length error-rate performance is comparable to list decoding of CRC-aided long polar codes while offering much lower memory-complexity implementation options.

## I. INTRODUCTION

THE polar code of [1] achieves capacity of the symmetric binary-input discrete memoryless channel while retaining a highly regular structure. In [1], a specific code utilizing the polarization effect coupled with a low-complexity successive cancellation (SC) decoder has been suggested. However, the demonstrated correction capability of the polar codes with finite code length is typically inferior to other known capacity-approaching codes such as low-density parity-check (LDPC) and turbo codes. For improving correction performance, several ways of concatenated coding and improved decoding have been proposed. Among all prior works, SC with list decoding appears most promising. In [2] and [3], the authors show that impressive correction capability can be achieved by applying list decoding to an SC decoder. Unlike conventional SC decoding with single-path-based search, up to  $L$  most likely paths are kept during decision steps in SC list (SCL) decoding, and the error rate performance of finite-length polar codes becomes close to that of the maximum likelihood (ML) decoder. Moreover, with additional cyclic-redundancy-check (CRC) coding, performance becomes comparable to LDPC codes.

This work is in part supported by the National Research Foundation of Korea under Grant No. 2016R1A2B4011298, and in part supported by the ICT R&D program of MSIP/IITP [2016-0-00563, Research on Adaptive Machine Learning Technology Development for Intelligent Autonomous Digital Companion].

The issue, however, is that multiple paths in SCL decoding lead to unavoidable memory burden. The required memory and computational burdens of SCL decoding with  $L$  paths of an  $N$ -bit-length polar code are  $O(LN)$  and  $O(LN \log N)$ , respectively [3]. Also in hardware synthesis [4], almost 90% of the overall size of the SCL decoder is dedicated to memory and the memory size increases linearly with the list size. This observation suggests that employing multiple short polar codes and finding a good concatenation strategy might be a way to reduce memory-burden while retaining acceptable performance

There are some known polar codes based on concatenation of multiple short polar codes. In [5], messages of multiple row-wise short non-systematic polar codes are encoded by multiple column-wise Reed-Solomon (RS) codes. At each bit-decision of the SC polar decoder, collection of the decision bits construct a single RS codeword. All parallel SC decoders output bits and wait until the RS decoder correct erroneous decisions. In [6], the outer Bose-Chaudhuri-Hocquenghem (BCH) codes and the convolutional codes are considered instead of the RS codes. For these schemes, all component SC decoders should make decisions bit-by-bit in a synchronous fashion. Thus, decoding cannot be carried out serially by a single small decoding unit, and hardware complexity remains a major issue. Recently, multiple polar codes have been parallel concatenated with a single recursive systematic convolutional (RSC) code [7]. The component polar code can be decoded by utilizing a single small polar code decoder. However, each row polar code should be decoded in a soft-out (SO) manner, which requires a fair number of decoding iterations. Along with additional iterations between the component polar codes and the RSC code, the total number of decoding iterations is substantial. Moreover, a long RSC code requires large memory space.

In this paper, we devise a highly efficient polar code based a concatenated coding scheme utilizing the multiple short polar codes and the single-parity-check (SPC) codes. Our proposed coding scheme relieves the memory-complexity issue of the single SCL-CRC decoded polar code and other polar-based concatenated codes. Message bits are simply encoded

by multiple disjoint outer SPC codes and after interleaving multiple short inner polar codes are encoded systematically. Each component inner polar code can be decoded by a single small-size SC decoder due to the short length of the component codes. The error rates decay as fast as the long single polar codes when plotted against the code length, erasure probability or signal-to-noise ratio (SNR), while enjoying significantly lower memory-complexity. Due to the short-length aspect of the component polar codes, SCL-CRC decoding can be applied with moderate memory complexity. With the SCL-CRC-decoded inner polar codes, error-rate performance of our proposed coding scheme is comparable to a single long SCL-CRC-decoded polar code, which exhibits the best performance to date among all known polar codes. Our theoretic analysis reveals that by simple concatenation of the outer SPC codes, the inner component polar codes show much improved error-rate scaling-behavior compared to the equal-length stand-alone polar codes and comparable behavior to much longer stand-alone polar codes.

## II. PROPOSED POLAR-SPC CONCATENATED CODES

### A. Encoding

*SPC encoding step:* For a given set of  $K$  message bits, divide it into  $k_c$  groups of size of  $K/k_c$  bits each. Then for each group, encode with a SPC code by appending a single parity bit, which is a result of an XOR operation on the message bits. After that, apply bit-wise random interleaving over all such SPC codewords.

*Row-wise polar code encoding step:* For the interleaved  $(K + k_c)$  SPC-coded bits, divide them into  $k_r$  groups. Each group can be visualized as constructing a row. Let us encode each row by a CRC code with  $p_{\text{crc}}$  parities and encode the resulting CRC codeword with a systematic polar code. Each row now represents a CRC-aided polar codeword with length  $N_r = (K + k_c)/k_r + p_{\text{crc}} + p_{\text{row}}$  bits, where  $p_{\text{row}}$  is the number of parity bits in each polar codeword. By the structure of the polar codes,  $N_r = 2^{n_r}$ , where  $n_r$  is a positive integer. Let us denote the CRC-aided polar code by *row-wise inner polar code*. Consequently, an encoded  $(k_r \times N_r)$ -bit array is obtained. The overall code-length  $N$  and the rate  $R$  are:

$$N = k_r N_r \text{ and } R = R_c (R_r - p_{\text{crc}}/N_r), \quad (1)$$

where  $R_c$  and  $R_r$  are the rates of the SPC and polar codes, respectively. Moreover, the following relationships should hold:

$$K = k_c N_c = k_r (R_r - p_{\text{crc}}/N_r) N_r \simeq k_r R_r N_r \quad (2)$$

where  $N_c$  is the SPC codeword length. Let us call the proposed code the *polar-SPC-concatenated code*. For helpful visualization of the code structure, consider a  $N_c = k_r$  case. The code structure is depicted in Fig. 1. Before interleaving, each of the first  $K/N_c$  columns forms a SPC codeword. After encoding the outer SPC codes and interleaving (which is not shown), row-wise CRC-aided polar coding is applied; a  $(k_r \times N_r)$ -bit coded array results.

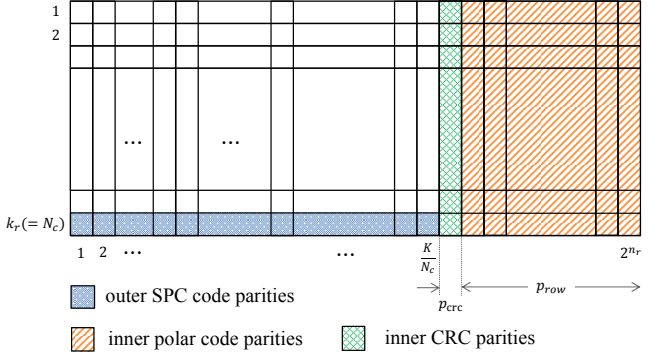


Fig. 1: Structure of the proposed polar-SPC concatenated code

### B. Decoding

Our proposed decoding is based on row-wise inner polar code decoding and column-oriented outer SPC code decoding. The inner and outer decoding steps are done in an iterative manner.

*Row-wise inner polar decoding turn:* Upon channel observation, decoding of row-wise inner CRC-aided polar codes proceeds. Each CRC-aided polar code is decoded by SC or SCL decoding in a row-by-row manner. After SC or SCL decoding, if a row decoder finds valid codeword by CRC checking, the corresponding decisions become the final outputs, i.e., plus or minus infinities in log-likelihood ratio (LLR) form. If all rows are successfully decoded, overall decoding is terminated with corresponding decisions. Otherwise, for failed row polar codes, collect their row indices in a set  $U_i$ . The subscript  $i$  means that the set is obtained after the  $i^{\text{th}}$  turn of inner/outer decoding iteration. If  $U_i$  is not an empty set, the LLR values captured in the  $(k_r \times N_r)$  array other than the CRC and polar parity portions are de-interleaved for the subsequent SPC decoding turn.

*Outer SPC decoding turn:* After the  $i^{\text{th}}$  row-wise inner decoding turn, each outer SPC codeword is decoded. Simple belief-propagation is applied to update the corresponding LLRs of each SPC codeword. After the one-shot LLR updates by the single parity bit, the array of the LLR values are again interleaved for the additional row-wise inner decoding turn.

*Additional row-wise inner decoding and iterative process:* After the outer SPC decoding turn, row-wise inner polar decoding at the  $(i+1)^{\text{th}}$  iteration is done only for rows whose indices are in  $U_i$ . Even with the additional row-wise inner decoding turn, failed rows can still persist. Denote the set of the indices of these persistent rows as  $U_{i+1}$ . If  $U_{i+1} = U_i$ , the overall decoding process is terminated and decoding failure is declared. If  $|U_{i+1}| \neq |U_i|$ , then an additional outer SPC decoding turn is triggered again. If  $U_{i+1}$  becomes empty, then we return the resulting decisions and declare a decoding success. Unless the decoding process meets these termination conditions, inner and outer decoding are repeated iteratively until the number of processed row decoding turns reaches  $I_{\max}$ .

### III. SCALING BEHAVIOR ANALYSIS OF PROPOSED POLAR-SPC CONCATENATED CODES

In this section, based on prior analysis of the scaling-law behavior for the SC-decoded single polar codes, the scaling-behavior of the word-error-rate (WER) lower-bound for the proposed polar-SPC-concatenated codes is examined. Our analysis is limited to the binary-erasure-channel (BEC) case but it will provide significant theoretic insights into improved scaling-behavior of our polar-SPC concatenated codes in general channel settings as well.

#### A. Posteriori Information between Row-wise Inner Polar and Outer SPC codes

For the BEC, erasures coming from previous row decoding turn can be partially corrected by outer SPC decoding. Let us assume that  $n_e$  rows fail after 1<sup>st</sup> row-decoding-turn. For the remaining erasures on the failed rows, de-interleaving shuffles the erasures and spread them into  $k_c$  SPC codewords. Let us focus on the statistical behavior of the number of erasures on each SPC codeword. For the number of erasures on each SPC codeword, its probability density function converges to a very simple form of distribution with sufficiently large  $N_r$ . A prior work tackles a related mathematical problem of allocating balls into boxes [8]. This prior work establishes the following facts.

*Strong-law of allocation* [8]: Let us place  $m_n$  balls successively into  $k_n$  boxes. Assume that each placement is identical, independent and equi-probable. Denote  $\mathbf{I}_{k_n m_n i}^{(r)}$  as the indicator of  $i^{th}$  box containing exactly  $r$  balls after all  $m_n$  balls are placed. The number of boxes containing exactly  $r$  balls can be represented as  $\mu_n = \sum_{i=1}^{k_n} \mathbf{I}_{k_n m_n i}^{(r)}$ . If  $\frac{m_n}{k_n} \rightarrow \lambda$  as  $n \rightarrow \infty$ , then  $\frac{\mu_n}{k_n} \rightarrow e^{-\lambda} \lambda^r / r!$  almost surely.

We can now approximate the number of remaining erasures after SPC decoding turn. In our case, there are  $k_c = k_r R_r N_r / N_c$  SPC codewords. With an ideal random interleaver and corresponding de-interleaver, erasures are highly spread into column codewords. Let us denote  $N_e$  as the number of erasures on  $n_e$  failed rows and  $\lambda$  as the ratio of  $N_e$  to  $k_c$ . Then for a fixed code rate of SPC and inner polar coding, the following convergence behaviors are valid as  $N_r \rightarrow \infty$ .

$$N_e / N_r \rightarrow \epsilon n_e R_r \text{ and } \lambda \rightarrow \epsilon n_e N_c / k_r. \quad (3)$$

The first convergence is from the *law of large numbers* for the number of erasures from the BEC. If we denote  $\mu_k$  as the number of SPC codewords containing  $k$  erasures, according to the *strong-law of allocation* in [8], the ratio of such codewords can be approximated as

$$\frac{\mu_k}{k_c} \rightarrow e^{-\epsilon n_e \frac{N_c}{k_r}} \frac{(\epsilon n_e \frac{N_c}{k_r})^k}{k!} \quad (4)$$

as  $N_r \rightarrow \infty$ . If a SPC codeword contains only one erasure, the erasure is correctable by simple SPC erasure decoding. We can formulate the convergence of the overall number of

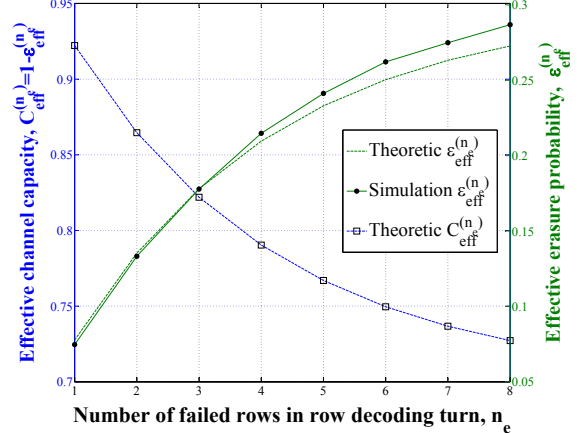


Fig. 2: Effective erasure probability  $\epsilon_{\text{eff}}^{(n_e)}$  for BEC( $\epsilon = 0.30$ )

corrected erasures  $\Delta N_e$  divided by  $N_r$  as

$$\frac{\Delta N_e}{N_r} \rightarrow \frac{k_r R_r}{N_c} \epsilon n_e \frac{N_c}{k_r} e^{-\epsilon n_e \frac{N_c}{k_r}} = \epsilon n_e R_r e^{-\epsilon n_e \frac{N_c}{k_r}} \quad (5)$$

as  $N_r \rightarrow \infty$ . Consequently, for the remaining erasures after SPC decoding,  $N'_e$ , we can formulate the convergence of  $N'_e / N_r$ . Moreover, we can define the *effective erasure-probability*  $\epsilon_{\text{eff}}^{(n_e)}$  after SPC decoding turn.

$$\frac{N'_e}{N_r} \triangleq \frac{N_e - \Delta N_e}{N_r} \rightarrow \epsilon n_e R_r (1 - e^{-\epsilon n_e \frac{N_c}{k_r}}) \triangleq \epsilon_{\text{eff}}^{(n_e)} n_e R_r, \quad (6)$$

where

$$\epsilon_{\text{eff}}^{(n_e)} = \epsilon (1 - e^{-\epsilon n_e \frac{N_c}{k_r}}). \quad (7)$$

Note that the analysis is based on the following assumptions.

*Assumption 1:* The number of erasures from the failed rows is assumed to follow the law of large numbers with BEC( $\epsilon$ ).

*Assumption 2:* Random interleaving is modeled as an identical, independent and equi-probable allocation problem.

However, the failed rows are actually from the failed-to-decode samples of the SC or SCL decoder. Moreover, random interleaving is not exactly equi-probable consecutive allocation. Actual samples are gathered from simulated  $n_e$  failed rows to confirm whether these assumptions are valid.

In Fig. 2, we consider a proposed polar-SPC code of length  $N = 8192$  bits and rate  $R = 0.50$  with  $k_r = 8$  component polar codes of length  $N_r = 1024$  bits and rate  $R_r = 0.579$ . For SPC coding,  $N_c = 8$ -bit-long SPC codes are considered. We can easily see that the formulated  $\epsilon_{\text{eff}}^{(n_e)}$  is a good approximation to the real values unless  $n_e$  gets large. Difference between analysis and simulation at large  $n_e$  comes from *Assumption 2* based on ideal allocation. In Fig. 3, the actual distribution of erasures on SPC-coded area per row is examined. The code parameters and channel condition are the same as in Fig. 2. The rightmost (gray) distribution is the initial number of erasures per failed row polar codeword. Two remaining distributions are the numbers of erasures after

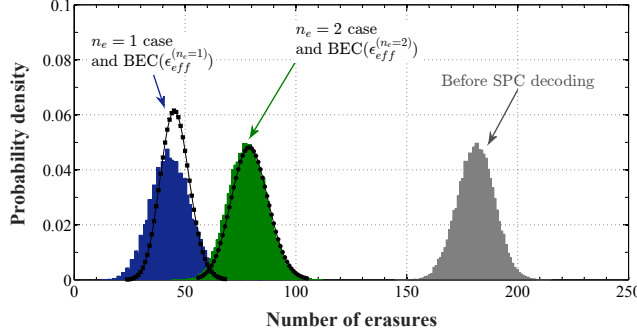


Fig. 3: Real probability density functions (pdfs) of the number of erasures before/after SPC decoding and the corresponding  $\text{BEC}(\epsilon_{\text{eff}}^{(n_e)})$  pdfs

SPC decoding for  $n_e = 1$  (blue) and  $n_e = 2$  (green) from left to right. With these actual distributions, the corresponding  $\text{BEC}(\epsilon_{\text{eff}}^{(n_e)})$  probability densities are also presented. The actual distributions are shown to be wider than  $\text{BEC}(\epsilon_{\text{eff}}^{(n_e)})$  but are in good agreement in mean values. These actual distributions are approximated to the BEC-model for rough WER performance analysis.

#### B. Scaling-law Behavior of the Proposed Coding Scheme

In [9] and [10], an approximate WER of the SC-decoded polar code is formulated as

$$P_e^{\text{sc}}(n, R, C) \simeq 2^{-2\frac{n}{2} + \sqrt{n}Q^{-1}(\frac{R}{C}) + o(\sqrt{n})}, \quad (8)$$

where  $n = \log_2 N$  and  $Q(t) \triangleq \int_t^\infty e^{-z^2/2} dz / \sqrt{2\pi}$ . The  $o(\sqrt{n})$  term is negligible for large  $n$ . The dominant code-length-related term  $\frac{n}{2} = \frac{1}{2} \log_2 N$  describes the scaling-behavior of WER versus  $N$ . On the other hand, the ratio of the code rate to channel capacity appears in the inverse  $Q$ -function:  $Q^{-1}(R/C)$ .

Given our effective erasure-probability  $\epsilon_{\text{eff}}^{(n_e)}$ , we approximate the resulting effective channel as  $\text{BEC}(\epsilon_{\text{eff}}^{(n_e)})$  with *effective channel capacity*  $C_{\text{eff}}^{(n_e)} = 1 - \epsilon_{\text{eff}}^{(n_e)}$ . Based on the previous two assumptions as well as *Assumption 3* below, a lower bound for the scaling-behavior of each component polar code after the 1st inner/outer decoding iteration can be formulated as follows.

*Assumption 3:* Given  $n_e$  failed inner polar codes at the first row decoding turn, after the SPC decoding turn, assume that the statistical distribution of the remaining erasures on the message part of each failed row polar code follows that of BEC with erasure probability  $\epsilon_{\text{eff}}^{(n_e)} = \epsilon(1 - e^{-\epsilon n_e \frac{N_c}{k_r}})$ .

**Lemma 1.** Let  $N$  be the overall code-length of the polar-SPC code.  $N_r = N/k_r$  and  $R_r$  are the length and rate of each component polar code. For  $\text{BEC}(\epsilon)$ , if  $n_e$  rows fail at the first row SC decoding turn, then the approximate WER in the sense of (8) of the each failed component polar code at additional SC decoding turn is lower bounded by

$$P_e^{\text{sc}}(N_r, R_r, C_{\text{eff}}^{(n_e)}) \simeq 2^{-2\frac{1}{2} \log_2 N_r + \sqrt{\log_2 N_r} Q^{-1}(R_r / C_{\text{eff}}^{(n_e)})}. \quad (9)$$

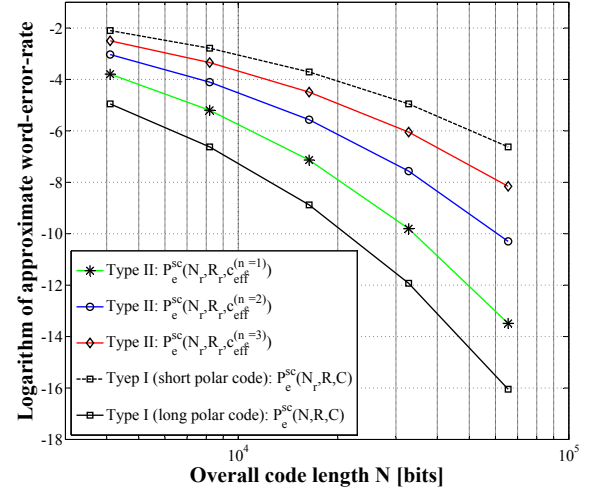


Fig. 4: Scaling-law behaviors of row component polar codes of the proposed concatenation after SPC decoding (Type II) and single polar codes (Type I)

*Proof.* We know that for a single polar code, the WER can be approximated by (8). By *Assumption 3*, the SPC-coded part of each failed row follows  $\text{BEC}(\epsilon_{\text{eff}}^{(n_e)})$ . We know that the parity part of each failed row is observed from the original channel  $\text{BEC}(\epsilon)$  where  $\epsilon_{\text{eff}}^{(n_e)} \leq \epsilon$ . Therefore, a lower bound for the WER of each failed inner polar code at additional row decoding turn can be formulated by substituting length  $N_r$ , rate  $R_r$  and channel capacity  $C_{\text{eff}}^{(n_e)} = 1 - \epsilon_{\text{eff}}^{(n_e)}$  to (8).  $\square$

In Fig. 4, Type I curves represent the single polar code with rate 0.5. One is of length  $N$  whereas the other (denoted “short polar code”) is of length  $N/8$ . These two curves are based on the approximate WER formula of (8). Type II curves are from (9) and represent the scaling-behavior of the row component polar codes of the polar-SPC code at the second row decoding turn. We set  $N_c = k_r = 8$ . The overall code length of the polar-SPC code is  $N$  bits but each component row polar code is 8 times shorter at  $N_r$  bits. An important observation in Fig. 4 is that the scaling-behavior of the row component polar code is shown to improve significantly by only simple column-wise SPC decoding. Even with much shorter code length  $N_r = N/k_r$  bits, the row component polar codes show WERs decaying at the same rate as the single long polar code of length  $N$ . Note that the  $n_e = 1$  case is dominant in the moderate and high SNR regimes.

For one iterative decoding process, a lower bound on the WER for an overall polar-SPC concatenated code  $P_e^{\text{conc}}$  can be formulated as follows. We denote  $P_e^{\text{sc}}(N_r, R_r, C) = P_{e,\text{inner}}^{\text{sc}}$  for simplicity.

$$\begin{aligned} & P_e^{\text{conc}}(N_r, k_r, R_r) \\ & \simeq \sum_{n_e=1}^{k_r} \left[ \binom{k_r}{n_e} (P_{e,\text{inner}}^{\text{sc}})^{n_e} (1 - P_{e,\text{inner}}^{\text{sc}})^{k_r - n_e} \right. \\ & \quad \left. \cdot \{1 - (1 - P_e^{\text{sc}}(N_r, R_r, C_{\text{eff}}^{(n_e)}))^n\}^{n_e} \right]. \end{aligned} \quad (10)$$

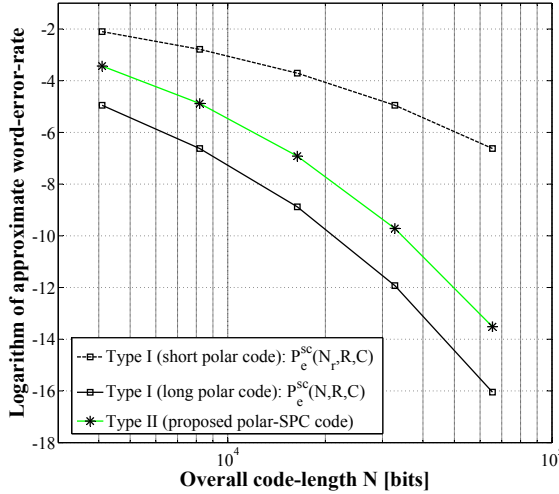


Fig. 5: Approximate WER scaling-behavior of the proposed polar-SPC code for  $\text{BEC}(\epsilon = 0.30)$

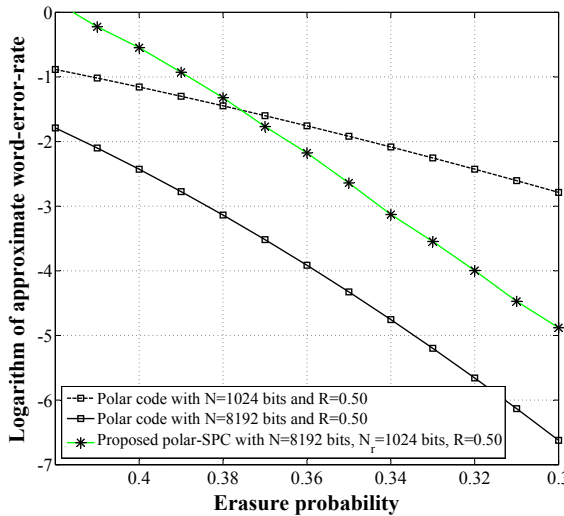


Fig. 6: Approximate WER of the proposed polar-SPC code versus erasure probability

Figs. 5 and 6 show the scaling-behavior of the overall polar-SPC concatenated code. As the overall code length increases, the lower bound on the WER of the polar-SPC code decays as rapidly as a long stand-alone polar code. A similar conclusion is drawn for the WERs plotted against channel erasure probability. Apparently, the effective erasure probability of (7) and thus the effective channel capacity can be expressed as functions of the number of iteration runs under the assumption that each decoding iteration/interleaving yields a BEC, which will show the improving scaling behavior with inner/outer decoding iterations. This formulation will be discussed elsewhere.

Note that using much shorter component polar codes, ample opportunities exist to reduce memory-complexity. From this point on, we use the approximate WER lower bound of (9) to

describe the scaling-behavior of the component polar codes.

#### IV. PARAMETER OPTIMIZATION AND NUMERICAL RESULTS

In this section, the error-rate performance and complexity issues of the proposed polar-SPC concatenated codes are considered. Before proceeding, we address coding parameter optimization first.

##### A. Coding Parameter Optimization

In this part, we present analysis for selecting code parameters which gives insights into the essential questions on the lengths and rates of the component codes.

*Number of row component polar codes  $k_r$ :* The number of the row-wise inner polar codes dominates the overall hardware-efficiency of the decoder, especially, the required memory size. we wish to make the number as large as possible (to make the component code shorter and reduce memory size) but being too large would hurt the performance. What is the ideal value of  $k_r$ ? In (8) and (9), focus on the terms in the exponents that depend on the code length  $N$ . Consider the following inequalities:

$$\begin{aligned} & \frac{1}{2} \log_2 N + \sqrt{\log_2 N} Q^{-1}(R/C) \\ & \leq \frac{1}{2} \log_2 (N/k_r) - \sqrt{\log_2 (N/k_r)} Q^{-1}(R_r/C_{\text{eff}}^{(n_e)}) \quad (11) \\ & \leq \frac{1}{2} \log_2 (N/k_r) - \sqrt{\log_2 (N/k_r)} Q^{-1}(R_r) \end{aligned}$$

The first inequality holds if the row component polar code of the polar-SPC code is to show a better scaling-behavior than the stand-alone long polar code. The second inequality results by substituting 1 for  $C_{\text{eff}}^{(n_e)}$ . The rightmost expression can be used to roughly estimate how much the row component polar code can be shortened while retaining reasonable scaling-behavior. Although the strategies for selecting  $R_r$  is not addressed yet, we can investigate the exponent values for a certain range of  $R_r$  above some fixed overall rate  $R$ .

In Fig. 7, for the given parameters  $N = 2048$  bits,  $R = 0.50$  and  $\text{BEC}(\epsilon = 0.35)$ , we investigate the maximum feasible  $k_r$  satisfying the inequality (11) with  $R_r$  ranging from 0.50 to 0.60. As  $k_r$  increases, each component polar code becomes shorter so that the corresponding exponent value decreases. The rightmost expression of (11) stays above the leftmost expression, a horizontal line, for all  $R_r$  values considered when  $k_r$  is less than or equal to 8. Thus,  $k_r = 8$  is a good value for the number of row component polar codes in view of guaranteeing better scaling-behavior for the row component polar code than the stand-alone long polar code of length 2048 bits.

*Code-rates of row polar and SPC codes:* Another main issue is about how the inner row and outer code-rates  $R_r$  and  $R_c$  should be set, for a fixed overall-rate  $R$ . In Fig. 8, we explore the scaling-behavior of the row inner component polar code for various  $N_c$  selections. The overall rate is fixed to  $R = 0.50$  and  $\text{BEC}(\epsilon = 0.30)$  is considered. With large  $N_c$ , which is equivalent to a high rate of outer SPC coding  $R_c$ , the

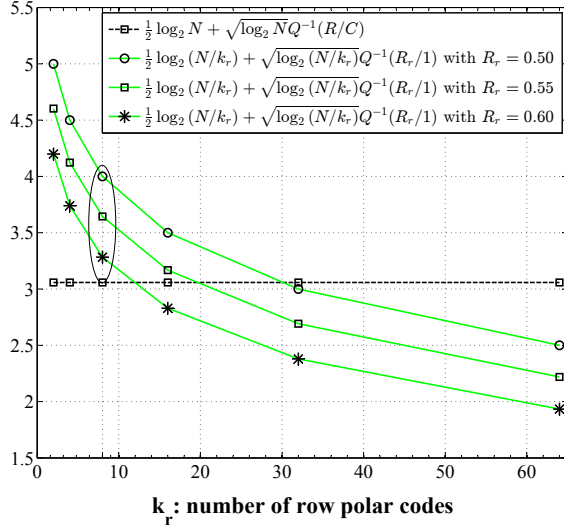


Fig. 7: Error exponent comparison of the component row polar code and the single long polar code

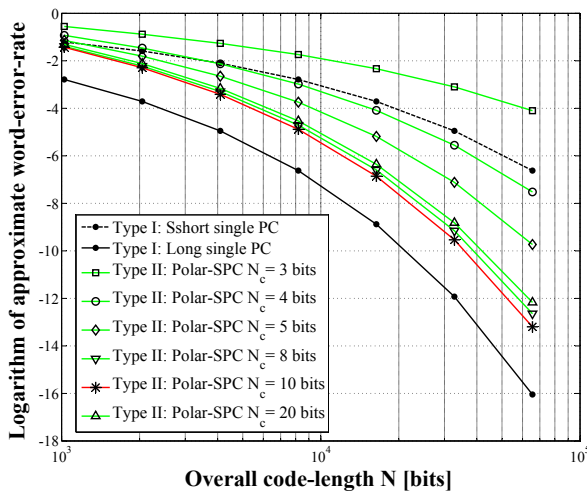


Fig. 8: Approximate WERs of the row component polar codes of the polar-SPC codes for various  $N_c$  settings

effective erasure probability increases but more parities can be allocated for each row-wise polar coding. On the other hand, as  $N_c$  decreases, fewer bits are collected in a SPC codeword so that  $R_c$  is decreased and effective erasure probability is also reduced. However, error-correction performance of each row polar code can be weakened due to an increased  $R_r$ . The figure shows what should be the appropriate selection of  $N_c$  for optimal scaling-behavior of each component polar code. For  $N_c$  much less than 10 bits,  $R_c$  is too low so that the row component polar code cannot offer an improved scaling-behavior compared with the single long polar code (denoted as Type I, long single PC). For  $N_c = 10$  bits, the component row polar code shows almost the same degree of WER decay as that of the long single polar code. Beyond this setting, the scaling-behavior starts to worsen due to overly weakened outer SPC codes. For the selected value  $N_c = 10$ ,  $R_r = 0.587$  and

$R_c = 0.90$  for  $N = 2048$  bits and  $R = 0.50$ . In practical code-parameter design, SPC-coded  $N_c k_c$  bits should be multiples of  $k_r$  so that there is a restriction on precise coding-parameter optimization. Therefore, for the numerical results to be shown later, we select  $N_c = 8$  bits rather than the optimal 10 bits. We can easily see that the scaling-behavior is not much different.

For showing deeper insights into rate optimization of row inner polar and outer SPC codes, we extend our outer SPC coding to general maximal distance separation (MDS) coding. We assume that the outer MDS codes have correction-capability up to  $p_{\text{col}}$  erasures where  $p_{\text{col}}$  is the number of parities. We fix  $N_c$  to moderate code length size and control the number of MDS parities  $p_{\text{col}}$ . The resulting code rate of the outer MDS code is  $R_c = (N_c - p_{\text{col}})/N_c$ . Although realization of binary MDS codes for given code length and rate is an open problem, let us assume  $N_c$ -bit-long outer MDS codes with  $p_{\text{col}}$  parities. By considering disjoint  $k_c = K/N_c$  outer MDS codes instead of SPC codes, the resulting effective erasure probability  $\epsilon_{\text{eff},\text{MDS}}^{(n_e)}$  can be formulated for given  $n_e$  failed rows:

$$\epsilon_{\text{eff},\text{MDS}}^{(n_e)} = \epsilon \left\{ 1 - e^{-\epsilon n_e \frac{N_c}{k_r}} \sum_{k=0}^{p_{\text{col}}-1} \frac{(\epsilon n_e \frac{N_c}{k_r})^k}{k!} \right\} \quad (12)$$

The details of formulation are analogous to the polar-SPC case and are omitted due to the lack of space. The summation from index 0 to  $p_{\text{col}} - 1$  corresponds to correction capability of the MDS code from single to  $p_{\text{col}}$  erasures. Although not shown, the corresponding scaling-behavior of the component short polar code improves substantially with the MDS codes. Another interesting possibility is to replace SPCs with multi-bit parity codes in the form of factor-graph-based code.

### B. Performance verification

In Fig. 9, bit-error-rate performance of length-1024, rate-1/2 polar-SPC concatenated codes and single long SC decoded polar codes are presented for BEC. For coding parameters,  $k_r = 8$  row polar codes with length 128 bits are concatenated with 8-bit-long outer SPC codes. CRC-8 is used and rates of the component codes are  $R_r = 0.634$  and  $R_c = 0.875$ . Moreover,  $I_{\max} = 8$ . We can easily see that polar-SPC with SC-decoded inner component polar codes shows the same degree of decaying slope as the stand-alone long SC-decoded polar code (denoted as ‘long PC’). Inner decoding of the polar-SPC can be done by a single 128-bit-long SC decoder (same as the short polar-code). When we introduce SCL-CRC decoding with list-8 for polar-SPC code, performance is significantly improved with 128-bit inner SCL( $L = 8$ )-CRC decoding which only requires memory-complexity at the same level as the 1024-bit-long SC decoder. Selection of frozen bits for all codes are optimized at BEC with  $\epsilon = 0.30$ .

In Fig. 10, an additive-white-Gaussian-noise (AWGN) channel is considered. Length and rate of polar-SPC is  $N = 2048$  bits and  $R = 0.50$ . The same parameters of  $k_r = 8$  and  $N_c = 8$  bits are considered.  $I_{\max} = 8$  for all polar-SPC codes. We observe that polar-SPC with SCL( $L = 32$ )-CRC inner decoding shows, surprisingly, comparable performance

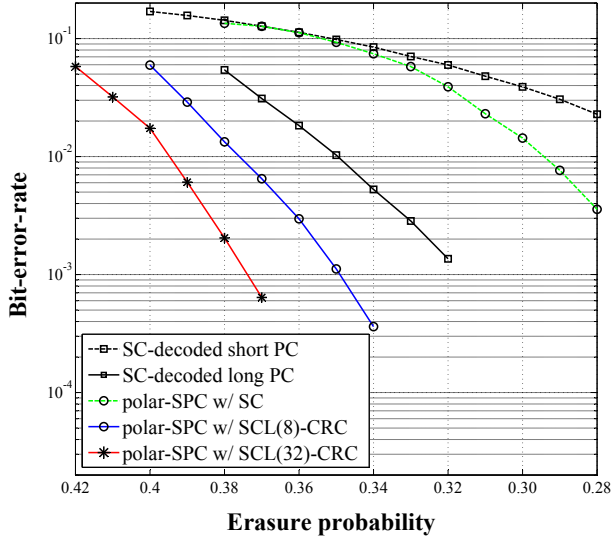


Fig. 9: Bit-error-rate performance of the polar-SPC code with  $N = 1024$  bits and  $R = 0.50$  for BEC

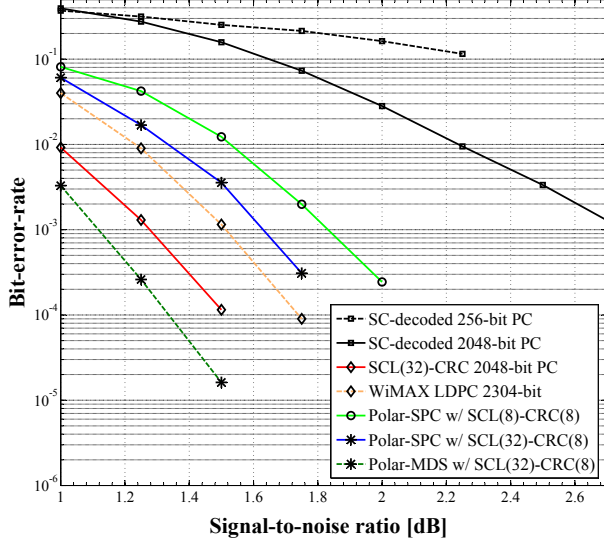


Fig. 10: Bit-error-rate performance of polar-SPC/MDS codes of length  $N = 2048$  bits and rate  $R = 0.50$  for AWGN channel

to that of SCL(32)-CRC decoded single PC that is  $k_r$ -times longer. With polar-SPC coding scheme, we can enjoy such improved correction performance with  $k_r$ -times reduced memory-complexity burden in the decoder unit. Finally, the polar-MDS codes with ideal MDS codes with  $N_c = 64$  and  $p_{col} = 8$  outperform the SCL(32)-CRC decoded long polar code, which is the best polar coding scheme reported to date. All polar codes are optimized at  $2.00\text{dB}$  as done in [11].

### C. Complexity analysis

With serialized SCL-CRC decoding of inner polar codes, the decoder requires  $O(LN_r)$  memory units and  $O(I_{max}(Lk_rN_r \log N_r + N))$  computations as respectively. In Table I, complexity of relevant prior coding schemes are compared to our proposed polar-SPC code. Memory and

TABLE I: Memory and computational complexity comparison

Coding schemes	Memory	Computation
Polar-SPC	$O(LN_r)$	$O(I_{max}(LN \log N_r + N))$
RS-polar [5]	$O(k_r N_r)$	$O(N(\log N)^2 \log \log N)$
Polar-RSC [7]	$O(2^v N)$	$O(I_1^{\max} N(I_2^{\max} \log N_r + 2^{v+1}))$
SCL-CRC PC [3]	$O(LN)$	$O(LN \log N)$

$v$ : number of state registers for RSC code

$I_1^{\max}$ : maximum number of iterations between polar and RSC decoder

$I_2^{\max}$ : maximum number of iterations for component polar decoder

computational complexity of polar-SPC is much lower than other codes with moderate  $L$  with impressive correction performance. The price paid for the serialized low-complexity hardware is latency, but compared to a long single polar code with list decoding, latency associated with list sorting is smaller with the proposed code.

## V. CONCLUSION

Polar-SPC concatenated codes with multiple short-length inner polar codes and outer SPC codes are suggested. Along with hardware-efficiency in memory requirement, the component polar code enjoys much improved scaling-behavior with the assistance of simple SPC decoding. Correction performance is comparable to the SCL-CRC-decoded long single polar code when list decoding of short inner polar codes is allowed.

## REFERENCES

- [1] E. Arikan, "Channel polarization: A method for constructing capacity achieving codes for symmetric binary-input memoryless channels," *IEEE Trans. Inf. Theory*, vol. 55, no. 7, pp. 3051-3073, Jul. 2009.
- [2] I. Tal and A. Vardy, "List decoding of polar codes," *IEEE International Symposium on Inf. Theory (ISIT)*, 2011.
- [3] I. Tal and A. Vardy, "List decoding of polar codes," *IEEE Trans. Inf. Theory*, vol. 61, no. 5, pp. 2213-2226, May 2015.
- [4] A. Balatsoukas-Stimming, M. B. Parizi and A. Burg, "LLR-based successive cancellation list decoding of polar codes," *IEEE Trans. Signal Processing*, vol. 63, no. 19, pp. 5165-5179, Oct. 2015.
- [5] H. Mahdavifar, M. El-Khamy, J. Lee and I. Kang, "Performance limits and practical decoding of interleaved reed-solomon polar concatenated codes," *IEEE Trans. Commun.*, vol. 62, no. 5, pp. 1406-1417, May 2014.
- [6] Y. Wang, K. R. Narayanan and Y. Huang, "Interleaved concatenations of polar codes with bch and convolutional codes," *IEEE Journal on Selected Areas in Commun.*, vol. 34, no. 2, pp. 267-277, Feb. 2016.
- [7] Q. Zhang, A. Liu, Y. Zhang and X. Liang, "Practical design and decoding of parallel concatenated structure for systematic polar codes," *IEEE Trans. Commun.*, vol. 64, no. 2, pp. 456-466, Feb. 2016.
- [8] A. Chuprunov, and I. Fazekas, "Inequalities and strong laws of large numbers for random allocations," *Acta Mathematica Hungarica*, 2005.
- [9] S. H. Hassani, R. Mori, T. Tanaka, and R. L. Urbanke, "Rate-dependent analysis of the asymptotic behavior of channel polarization," *IEEE Trans. Inf. Theory*, vol. 59, no. 4, pp. 2267-2276, Apr. 2013.
- [10] S. H. Hassani, K. Alishahi, and R. L. Urbanke, "Finite-length scaling for polar codes," *IEEE Trans. Inf. Theory*, vol. 60, no. 10, pp. 5875-5898, Oct. 2014.
- [11] I. Tal and A. Vardy, "How to construct polar codes," *IEEE Trans. Inf. Theory*, vol. 59, no. 10, pp. 6562-6582, Oct. 2013.